

Intrinsic device-to-device variation in graphene field-effect transistors on a Si/SiO₂ substrate as a platform for discriminative gas sensing

Alexey Lipatov, Alexey Varezchnikov, Martin Augustin, Michael Bruns, Martin Sommer, Victor Sysoev, Andrei Kolmakov, and Alexander Sinitskii

Citation: [Applied Physics Letters](#) **104**, 013114 (2014); doi: 10.1063/1.4861183

View online: <http://dx.doi.org/10.1063/1.4861183>

View Table of Contents: <http://scitation.aip.org/content/aip/journal/apl/104/1?ver=pdfcov>

Published by the [AIP Publishing](#)

Articles you may be interested in

[Publisher's Note: "Intrinsic device-to-device variation in graphene field-effect transistors on a Si/SiO₂ substrate as a platform for discriminative gas sensing" \[Appl. Phys. Lett. 104, 013114 \(2014\)\]](#)

[Appl. Phys. Lett.](#) **104**, 149902 (2014); 10.1063/1.4864791

[pH sensing properties of graphene solution-gated field-effect transistors](#)

[J. Appl. Phys.](#) **114**, 084505 (2013); 10.1063/1.4819219

[Graphene based field effect transistor for the detection of ammonia](#)

[J. Appl. Phys.](#) **112**, 064304 (2012); 10.1063/1.4752272

[Detection of sulfur dioxide gas with graphene field effect transistor](#)

[Appl. Phys. Lett.](#) **100**, 163114 (2012); 10.1063/1.4704803

[Probing transconductance spatial variations in graphene nanoribbon field-effect transistors using scanning gate microscopy](#)

[Appl. Phys. Lett.](#) **100**, 033115 (2012); 10.1063/1.3678034

An advertisement for KeySight B2980A Series Picoammeters/Electrometers. The ad features a red and white color scheme. On the left, text reads 'Confidently measure down to 0.01 fA and up to 10 PΩ' and 'KeySight B2980A Series Picoammeters/Electrometers'. Below this is a red button with the text 'View video demo'. On the right, there is an image of the device and the KeySight Technologies logo.

Intrinsic device-to-device variation in graphene field-effect transistors on a Si/SiO₂ substrate as a platform for discriminative gas sensing

Alexey Lipatov,¹ Alexey Varezchnikov,² Martin Augustin,³ Michael Bruns,⁴ Martin Sommer,³ Victor Sysoev,² Andrei Kolmakov,^{5,a)} and Alexander Sinitskii^{1,6,b)}

¹Department of Chemistry, University of Nebraska–Lincoln, Lincoln, Nebraska 68588, USA

²Department of Physics, Saratov State Technical University, Saratov 410054, Russian Federation

³Institute of Microstructure Technology, Karlsruhe Institute of Technology (KIT),

Hermann-von-Helmholtz-Platz 1, 76344 Eggenstein-Leopoldshafen, Germany

⁴Institute for Applied Materials - Energy Storage Systems (IAM-ESS), Karlsruhe Institute of Technology (KIT),

Hermann-von-Helmholtz-Platz 1, 76344 Eggenstein-Leopoldshafen, Germany

⁵Department of Physics, Southern Illinois University, Carbondale, Illinois 62901, USA

⁶Nebraska Center for Materials and Nanoscience, University of Nebraska–Lincoln, Lincoln, Nebraska 68588, USA

(Received 12 September 2013; accepted 18 December 2013; published online 10 January 2014; publisher error corrected 15 January 2014)

Arrays of nearly identical graphene devices on Si/SiO₂ exhibit a substantial device-to-device variation, even in case of a high-quality chemical vapor deposition (CVD) or mechanically exfoliated graphene. We propose that such device-to-device variation could provide a platform for highly selective multisensor electronic olfactory systems. We fabricated a multielectrode array of CVD graphene devices on a Si/SiO₂ substrate and demonstrated that the diversity of these devices is sufficient to reliably discriminate different short-chain alcohols: methanol, ethanol, and isopropanol. The diversity of graphene devices on Si/SiO₂ could possibly be used to construct similar multisensor systems trained to recognize other analytes as well. © 2014 AIP Publishing LLC.

[<http://dx.doi.org/10.1063/1.4861183>]

Because of its excellent electrical properties, such as high conductivity and charge carrier mobilities, graphene is a promising material for future electronics.^{1–3} Graphene sheets are produced by different techniques, such as micromechanical cleavage,⁴ vacuum decomposition of SiC,⁵ chemical vapor deposition (CVD),^{6–8} carbon nanotube unzipping,^{9–11} and reduction of graphene oxide (GO),^{12,13} but regardless of the preparation method, significant device-to-device variations in its electron transport properties are often reported. For example, the conductivities of two-terminal devices based on individual monolayer flakes of a reduced GO (rGO) vary by at least an order of magnitude,^{14,15} and similar results have been reported for electronic devices based on graphene nanoribbons prepared by the oxidative unzipping of carbon nanotubes.^{16,17} Such device-to-device variations could be attributed to the fact that rGO has an irregular atomic structure that comprises nearly perfect graphene domains, oxidized regions, and nanoscopic holes.^{12,13} However, even for a much higher quality CVD-grown graphene, substantial device-to-device variations are also observed.^{18,19}

Graphene flakes prepared by a micromechanical exfoliation are commonly believed to have the highest structural quality compared to graphene samples prepared by other techniques.¹ However, Figure 1 shows that the device-to-device variations in arrays of field-effect transistors (FETs) based on graphene prepared by the micromechanical exfoliation⁴ and CVD could be comparable. Figure 1(a) shows an array of 25 two-terminal devices with CVD graphene channels and Cr/Au contacts (see supplementary material²⁰ for experimental

details on graphene growth and device fabrication). For comparison, we also fabricated four two-terminal devices based on a graphene flake prepared by the micromechanical exfoliation (Figure 1(b)). Both this flake and CVD graphene were monolayer, which was confirmed by Raman spectroscopy: all measured spectra exhibited narrow symmetric 2D bands centered at $\sim 2677\text{ cm}^{-1}$ and G-to-2D intensity ratios of $\sim 1:2$.²¹

Electrical measurements of graphene devices of both types were performed in vacuum after the devices were kept at a pressure of 3×10^{-6} Torr to minimize the doping effect of surface adsorbates.¹⁷ Figures 1(c) and 1(d) shows that FETs based on both CVD and exfoliated graphene exhibit a significant device-to-device variation. In case of the CVD graphene, devices with geometrically identical square ($15 \times 15\ \mu\text{m}^2$) channels and same Cr/Au contacts have different resistances in the range from 8 to 18 k Ω when measured without applying the gate voltage. Furthermore, the charge neutrality point (V_{NP} , point of the highest resistance) observed in the source-drain current (I_{sd})–gate voltage (V_g) curves (Figure 1(c)) is different for all 25 devices, ranging from -5 to 2 V (Figure 1(e)), which indicates a different charge doping level in these devices. The charge carrier mobilities also show a wide distribution, varying by nearly an order of magnitude—for example, at $V_g = 10$ V the hole mobilities range from 420 to 2630 $\text{cm}^2/\text{V}\cdot\text{s}$ for different devices in the array.

Device-to-device variation could be in part explained by the fact that the graphene grown by CVD is typically polycrystalline with misaligned domains separated by grain boundaries.^{22,23} Therefore, it is likely that different devices in this 5×5 array contained graphene channels with different defect concentrations, which is in agreement with the results of Raman spectroscopy. We have measured Raman

a) andrei.kolmakov@nist.gov

b) sinitskii@unl.edu

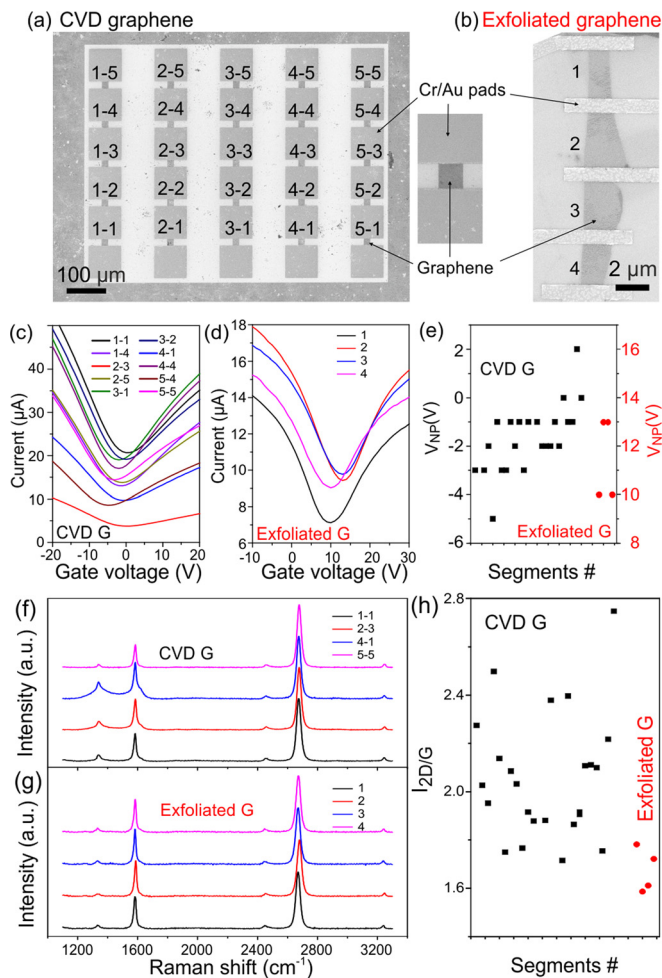


FIG. 1. (a) SEM image of an array of 25 devices based on a monolayer graphene grown by CVD. The inset shows SEM image of a typical device in this array. Numbers indicate the device numeration; same numbers are used in panels (c) and (f). (b) SEM image of four devices based on a monolayer sheet of a mechanically exfoliated graphene. (c) Transfer characteristics of ten representative devices based on a CVD graphene, see panel (a). (d) Transfer characteristics of four devices based on a mechanically exfoliated graphene, see panel (b). (e) V_{NP} values for different devices shown in panels (a) and (b). (f) Raman spectra of four representative devices based on a CVD graphene, see panel (a). (g) Raman spectra of four devices based on a mechanically exfoliated graphene, see panel (b). (h) 2D-to-G intensity ratios for Raman spectra for all devices shown in panels (a) and (b).

spectra for all 25 graphene devices in the array (four representative spectra are shown in Figure 1(f)) and found a significant variation in relative intensities of G, D, and 2D bands for different segments. In particular, we observed a strong D band for some of the segments, which is indicative of a high concentration of structural defects in graphene (Figure 1(f)). At the same time, in some graphene devices in the array the D band was barely visible (Figure 1(f)).

Thus, Raman spectra confirm that CVD graphene segments in the 5×5 array had different defect concentrations, which should contribute to the observed device-to-device variation (Figure 1(c)). However, a noticeable device-to-device variation (Figures 1(d) and 1(e)) was also observed for FETs based on higher quality exfoliated graphene segments (Figure 1(d)), for which the Raman spectra were nearly identical (Figures 1(g) and 1(h)). Therefore, these experiments show that a device-to-device variation in a graphene FET array cannot be solely explained by an intrinsic structural quality of graphene.

The extrinsic factors, such as non-uniform charge distribution on a surface of a Si/SiO₂ substrate,²⁴ graphene-metal contact effects,²⁵ and charged impurities²⁶ that could be caused by surface adsorbates²⁷ as well as by polymer residues,²⁸ could significantly contribute to the effect.

To illustrate the effect of the surface contamination on the device-to-device variation in graphene FETs we fabricated similar 5×5 arrays of FETs similar to the one shown in Figure 1(a), which were based on CVD graphene samples prepared using different Cu etchants, iron (III) chloride (FeCl₃) and potassium persulfate (K₂S₂O₈). Although FeCl₃ is a common Cu-based etchant used in the numerous studies of CVD graphene,²⁹ several reports indicate that persulfate etchants yield cleaner graphene samples.^{30,31} Graphene was grown by CVD on a 1×1 cm² Cu foil, which was then cut in two pieces, and graphene from one piece was transferred to Si/SiO₂ using FeCl₃ etchant, while graphene from another one was transferred to Si/SiO₂ using K₂S₂O₈ etchant (see supplementary material²⁰ for more details). Optical photographs of these samples show that graphene transferred using FeCl₃ etchant is indeed covered with surface contaminants, whereas graphene transferred using K₂S₂O₈ etchant looks much cleaner (Figures S1(a) and S1(b)²⁰). Accordingly, FETs fabricated from contaminated graphene, which was transferred using FeCl₃ etchant, exhibit a significant device-to-device variation, as the V_{NP} values for different devices range from -7 to >30 V (Figure S1(c)²⁰). In contrast, FETs fabricated from cleaner graphene, which was transferred using K₂S₂O₈ etchant, exhibit much smaller device-to-device variation (V_{NP} values range from 3 to 6 V; see Figure S1(d)²⁰). These results underscore the importance of a careful etching to minimize the variability of graphene FETs. Yet, even the FETs based on graphene transferred using K₂S₂O₈ etchant are not identical (see Figures 1(c) and S1(d)²⁰), which could be caused by the effect of Si/SiO₂ substrate.²⁴ Si/SiO₂ substrate is known to have a profound effect on the electronic properties of graphene since the charge carrier mobilities in graphene devices increase by an order of magnitude if graphene is suspended^{33,34} or placed on an atomically flat crystalline substrate.³² However, an interesting question is whether this device-to-device variation could actually be beneficial for certain applications.

In this Letter, we propose that variability in resistivity along the array of nearly identical graphene devices could be employed as a platform for selective gas detection.³³ According to the recent study by Kumar *et al.*, substrate defects have a strong effect on sensor properties of graphene devices.³⁴ Therefore, one can expect that multiple sensors based on graphene deposited on a Si/SiO₂ substrate should have variability in electronic sensor properties due to the stochastic substrate defects. An array of nonidentical sensors, for which the data are processed using pattern recognition algorithms could be considered as an electronic nose (*e-nose*; see reviews 35 and 36, and references therein). E-nose systems demonstrate very high selectivity in analyte recognition: although the intrinsic selectivity of a sensing material may be low, the combination of several segments in an array has a very large information content. An e-nose system is first calibrated to create a library of analytes of interest, and in the following recognition experiments the

measured analyte signals are compared with ones recorded in the library.³⁷ For the best performance of an e-nose system the segments of an array should exhibit a substantial variability in their sensor properties. Therefore, due to the discussed variability in properties of graphene devices on Si/SiO₂, an array of such devices appears to be a promising platform for an effective e-nose system.

In general, graphene-based gas sensors are known for their poor selectivity, although their sensitivity could be very high. It was demonstrated by Schedin *et al.* that individual graphene FETs could detect single events when a gas molecule attaches to or detaches from graphene's surface.²⁷ Since adsorption of acceptor molecules results in p-doping of graphene, whereas donor molecules cause n-doping, the FET measurement could be used to distinguish between donor and acceptor molecules.²⁷ But recognition of two molecules with similar (donor or acceptor) properties would be very challenging and may require additional characterization, such as the analysis of the low-frequency noise spectra.³⁸ As we demonstrate in this Letter, application of an e-nose concept to graphene sensors could be another approach to solve the selectivity problem.

As a platform for a graphene e-nose system, we employed a multielectrode KAMINA chip developed at Karlsruhe Institute of Technology (KIT),³⁹ see Figure 2(a). Previously, these multielectrode chips were successfully used in other studies of e-nose systems based on semiconductor nanomaterials^{39,40} and graphene oxide.⁴¹ The working part of the chip consists of a Si/SiO₂ substrate with 39 Pt electrodes wire-bonded to a ceramic frame (Figure 2(b)). A rectangular sheet of a monolayer CVD graphene was transferred to the Si/SiO₂ substrate thus forming 38 graphene devices with Pt electrodes (Figure 2(b)); each device (segment) in this array could be measured independently. Figure 2(c) shows *I-V* curves measured in air for all devices in the array. The linear character of these curves indicates Ohmic contacts between the CVD graphene and Pt

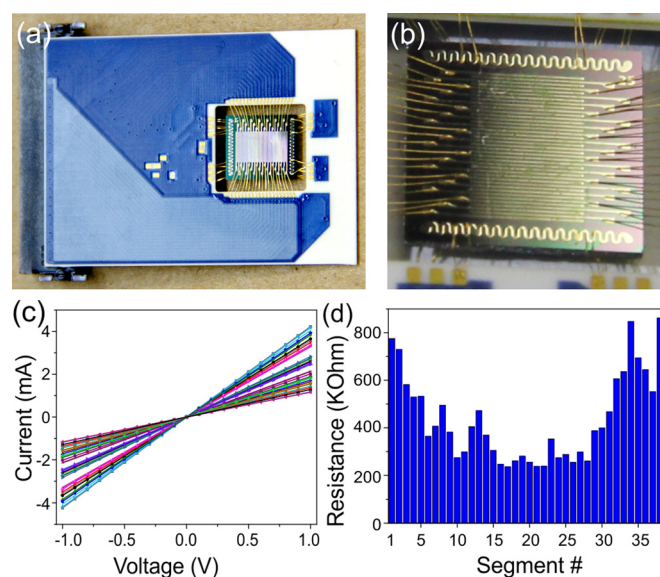


FIG. 2. (a) Optical photograph of a KAMINA chip. (b) Optical photograph of the working part of a KAMINA chip. Shown is a Si/SiO₂ substrate with 39 Pt electrodes that is covered with a rectangular monolayer sheet of a CVD graphene. (c) *I-V* curves measured in air for 38 graphene devices on a KAMINA chip shown in panel (b). (d) Distribution of resistances of 38 graphene devices on a KAMINA chip.

electrodes. Similar to the case of smaller devices fabricated by e-beam lithography and dry etching (Figure 1(a)) the segments of the multielectrode chip also exhibit a significant device-to-device variation. The segment resistances range from ~ 200 to >800 k Ω , and the resistance distribution is stochastic in nature (Figure 2(d)).

The device-to-device variability in graphene segments of the multielectrode chip is a key requirement for their use as an e-nose system. To demonstrate reproducible sensing and reliable recognition properties of the sensor array we tested its ability to discriminate between different short-chain alcohols, such as methanol, ethanol and isopropanol. Because of the high toxicity of methanol, it is practically important to reliably distinguish it from other alcohols. However, due to the similar chemical nature of these analytes, it would be challenging to reliably recognize them using a single graphene sensor. The experiments were performed in a nearly practical environment, i.e., under atmospheric pressure, in a dry air background and at room temperature.

Gas sensing measurements were performed using a custom-built gas system that is schematically shown in Figure 3(a) and described in detail in the Experimental section.²⁰ Briefly, the system contains two parallel gas lines with independent mass flow controllers (MFCs). When the gas valve is open, the graphene segments of the multielectrode chip are exposed to the flow of an analyte at a certain

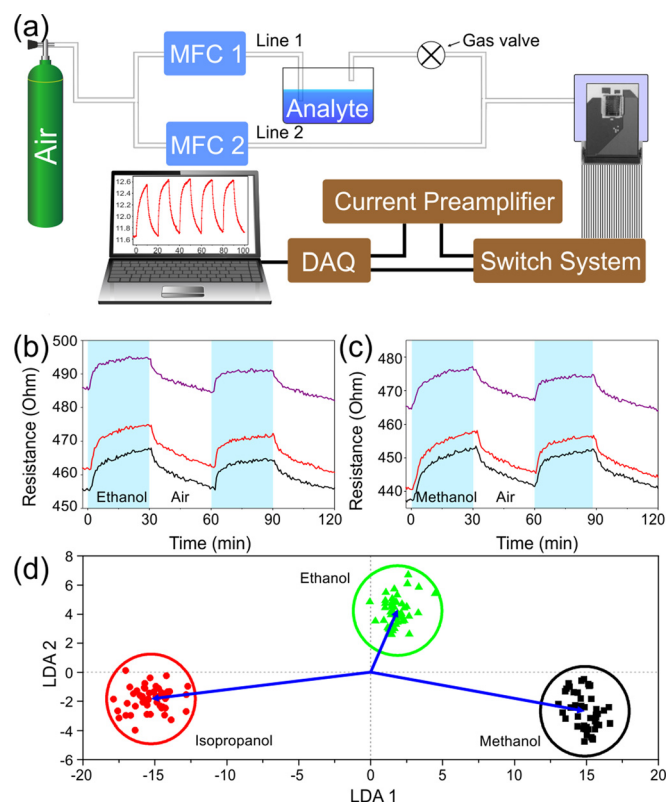


FIG. 3. (a) Experimental setup for sensor measurements (MFC—mass flow controller; DAQ—data acquisition system); see supplementary material²⁰ for experimental details. (b) and (c) Representative dynamic behaviors of three different graphene segments in the multielectrode chip, exposed to 1000 ppm of (b) ethanol and (c) methanol in synthetic air. (d) Results of the LDA processing of the sensor data generated by 38 graphene devices in a multielectrode system in different recognition experiments; see text for details. Vectors indicate the distances from the origin of the coordinate system to the centers of clusters corresponding to different analytes (methanol, ethanol, and isopropanol).

concentration; when the gas valve is closed, the devices are purged with a synthetic air (Figure 3(a)). The devices in the array are measured in series using a switch system; all 38 devices were measured within 15 s.

The sensing experiments show that the resistances of graphene segments of the multielectrode chip reproducibly change upon the exposure to different analytes. When a device is exposed to an alcohol vapor the resistance increases, whereas a purge with a synthetic air results in the resistance decrease (Figures 3(b) and 3(c)). While this behavior is only shown for three selected devices upon their exposure to ethanol (Figure 3(b)) or methanol (Figure 3(c)), it has been observed for all 38 segments when they were exposed to all three analytes. We observed a significant baseline drift after the first “exposure-purge” cycle, which is rather typical for other gas sensors based on different nanomaterials,⁴² but in the following cycles, the baseline was stable. The response and recovery time are in the order of minutes, which are determined by the employed gas delivery system and as well as low operating temperature and corroborates with prior data on graphene based sensors.⁴³ These characteristics still could be improved further via employing higher operating temperatures, and/or using catalysts, etc. Most importantly, the 38 segments of the multielectrode chip that exhibited a significant device-to-device variation in their electrical properties (Figure 2(d)) also differ in their responses to the tested short-chain alcohols. The responses of individual segments to different analytes deviate from each other both in their magnitude and response time (Figures 3(b) and 3(c)). As we discussed above, these variations could be caused not only by the structural non-uniformity of CVD graphene, but also by the stochastic defects that are present on the surface of an amorphous SiO₂ substrate.

The observed differences in sensor responses for 38 graphene segments of the multielectrode chip are large enough to allow the reliable discrimination of methanol, ethanol and isopropanol at a concentration of 1000 ppm. We processed the sensor responses excluding the first “exposure-purge” cycle by the pattern recognition technique based on Linear Discriminant Analysis (LDA).⁴⁴ This technique transfers the multidimensional sensor signals to a reduced two-dimensional space where the sensor responses of 38 graphene segments are grouped into separate clusters representing different analytes; the distances between vectors corresponding to different clusters are maximized to ensure reliable gas recognition. Figure 3(d) shows the results of the LDA processing of the data from the graphene-based multielectrode chip with the confidence probability of 0.99, demonstrating the capability of this sensor array to reliably discriminate the short-chain alcohols used in this study.

An array of graphene devices could recognize different alcohols due to the discussed device-to-device variability, and not due to any specific selectivity of graphene to alcohol adsorbates. Therefore, the same diversity of graphene devices on Si/SiO₂ could be the basis for e-nose systems trained to recognize other analytes as well. In general, e-nose systems benefit from larger numbers of segments and/or their higher diversity. An additional diversity could be introduced to the system, for example, through a selective chemical functionalization of some graphene devices in the array

using diazonium chemistry,^{45,46} which might be a promising direction for future studies.

In summary, we have demonstrated that arrays of graphene devices on Si/SiO₂ exhibit a substantial device-to-device variation, even if they have the same dimensions, contact materials, and are based on a high-quality CVD or mechanically exfoliated graphene. Such device-to-device variation is a potentially negative factor for large-scale graphene-based circuits, but as we demonstrate in this Letter, it could be beneficial for sensor applications. In a proof-of-concept experiment, we have fabricated an array of 38 graphene devices on a Si/SiO₂ substrate, and demonstrated that the diversity of these devices is sufficient to reliably discriminate three different short-chain alcohols: methanol, ethanol, and isopropanol. Such selectivity would be difficult to achieve for an individual graphene-based sensor. Arrays of graphene devices with a high diversity could possibly be trained to recognize not only different alcohols but other analytes as well. Further research could also be focused on the miniaturization of graphene multielectrode gas sensors and increasing the diversity of different segments through selective chemical functionalization.

The work at UNL was funded by the Nebraska Public Power District through the Nebraska Center for Energy Sciences Research (#12-00-13) and the NSF through Nebraska MRSEC (DMR-0820521) and EPSCoR (EPS-1004094). The research at SIUC was supported through the NSF ECCS-0925837 grant. V.S. and A.V. thank the partial support from the Russian Ministry of Education and Science grant #14.B37.21.1076.

¹A. K. Geim and K. S. Novoselov, *Nature Mater.* **6**, 183 (2007).

²K. S. Novoselov, V. I. Fal'ko, L. Colombo, P. R. Gellert, M. G. Schwab, and K. Kim, *Nature* **490**, 192 (2012).

³Y. M. Lin, C. Dimitrakopoulos, K. A. Jenkins, D. B. Farmer, H. Y. Chiu, A. Grill, and P. Avouris, *Science* **327**, 662 (2010).

⁴K. S. Novoselov, A. K. Geim, S. V. Morozov, D. Jiang, Y. Zhang, S. V. Dubonos, I. V. Grigorieva, and A. A. Firsov, *Science* **306**, 666 (2004).

⁵C. Berger, Z. M. Song, T. B. Li, X. B. Li, A. Y. Ogbazghi, R. Feng, Z. T. Dai, A. N. Marchenkov, E. H. Conrad, P. N. First, and W. A. de Heer, *J. Phys. Chem. B* **108**, 19912 (2004).

⁶A. N. Obratsov, E. A. Obratsova, A. V. Tyurnina, and A. A. Zolotukhin, *Carbon* **45**, 2017 (2007).

⁷A. Reina, X. T. Jia, J. Ho, D. Nezich, H. B. Son, V. Bulovic, M. S. Dresselhaus, and J. Kong, *Nano Lett.* **9**, 30 (2009).

⁸X. S. Li, W. W. Cai, J. H. An, S. Kim, J. Nah, D. X. Yang, R. Piner, A. Velamakanni, I. Jung, E. Tutuc, S. K. Banerjee, L. Colombo, and R. S. Ruoff, *Science* **324**, 1312 (2009).

⁹D. V. Kosynkin, A. L. Higginbotham, A. Sinitiskii, J. R. Lomeda, A. Dimiev, B. K. Price, and J. M. Tour, *Nature* **458**, 872 (2009).

¹⁰L. Y. Jiao, L. Zhang, X. R. Wang, G. Diankov, and H. J. Dai, *Nature* **458**, 877 (2009).

¹¹D. V. Kosynkin, W. Lu, A. Sinitiskii, G. Pera, Z. Z. Sun, and J. M. Tour, *ACS Nano* **5**, 968 (2011).

¹²D. R. Dreyer, S. Park, C. W. Bielawski, and R. S. Ruoff, *Chem. Soc. Rev.* **39**, 228 (2010).

¹³A. Sinitiskii and J. M. Tour, in *Graphene Nanoelectronics*, edited by R. Murali (Springer, New York, 2012), p. 205.

¹⁴C. Gomez-Navarro, R. T. Weitz, A. M. Bittner, M. Scolari, A. Mews, M. Burghard, and K. Kern, *Nano Lett.* **7**, 3499 (2007).

¹⁵D. C. Marcano, D. V. Kosynkin, J. M. Berlin, A. Sinitiskii, Z. Z. Sun, A. Slesarev, L. B. Alemany, W. Lu, and J. M. Tour, *ACS Nano* **4**, 4806 (2010).

¹⁶A. Sinitiskii, A. A. Fursina, D. V. Kosynkin, A. L. Higginbotham, D. Natelson, and J. M. Tour, *Appl. Phys. Lett.* **95**, 253108 (2009).

- ¹⁷A. Sinitskii, A. Dimiev, D. V. Kosynkin, and J. M. Tour, *ACS Nano* **4**, 5405 (2010).
- ¹⁸X. S. Li, C. W. Magnuson, A. Venugopal, J. H. An, J. W. Suk, B. Y. Han, M. Borysiak, W. W. Cai, A. Velamakanni, Y. W. Zhu, L. F. Fu, E. M. Vogel, E. Voelkl, L. Colombo, and R. S. Ruoff, *Nano Lett.* **10**, 4328 (2010).
- ¹⁹E. Pembroke, G. D. Ruan, A. Sinitskii, D. A. Corley, Z. Yan, Z. Z. Sun, and J. M. Tour, *Nano Res.* **6**, 138 (2013).
- ²⁰See supplementary material at <http://dx.doi.org/10.1063/1.4861183> for experimental details.
- ²¹A. C. Ferrari, J. C. Meyer, V. Scardaci, C. Casiraghi, M. Lazzeri, F. Mauri, S. Piscanec, D. Jiang, K. S. Novoselov, S. Roth, and A. K. Geim, *Phys. Rev. Lett.* **97**, 187401 (2006).
- ²²P. Y. Huang, C. S. Ruiz-Vargas, A. M. van der Zande, W. S. Whitney, M. P. Levendorf, J. W. Kevek, S. Garg, J. S. Alden, C. J. Hustedt, Y. Zhu, J. Park, P. L. McEuen, and D. A. Muller, *Nature* **469**, 389 (2011).
- ²³K. Kim, Z. Lee, W. Regan, C. Kisielowski, M. F. Crommie, and A. Zettl, *ACS Nano* **5**, 2142 (2011).
- ²⁴J. Martin, N. Akerman, G. Ulbricht, T. Lohmann, J. H. Smet, K. Von Klitzing, and A. Yacoby, *Nat. Phys.* **4**, 144 (2008).
- ²⁵F. N. Xia, V. Perebeinos, Y. M. Lin, Y. Q. Wu, and P. Avouris, *Nat. Nanotechnol.* **6**, 179 (2011).
- ²⁶J. H. Chen, C. Jang, S. Adam, M. S. Fuhrer, E. D. Williams, and M. Ishigami, *Nat. Phys.* **4**, 377 (2008).
- ²⁷F. Schedin, A. K. Geim, S. V. Morozov, E. W. Hill, P. Blake, M. I. Katsnelson, and K. S. Novoselov, *Nature Mater.* **6**, 652 (2007).
- ²⁸M. Ishigami, J. H. Chen, W. G. Cullen, M. S. Fuhrer, and E. D. Williams, *Nano Lett.* **7**, 1643 (2007).
- ²⁹C. Mattevi, H. Kim, and M. Chhowalla, *J. Mater. Chem.* **21**, 3324 (2011).
- ³⁰B. Aleman, W. Regan, S. Aloni, V. Altoe, N. Alem, C. Girit, B. S. Geng, L. Maserati, M. Crommie, F. Wang, and A. Zettl, *ACS Nano* **4**, 4762 (2010).
- ³¹J. W. Suk, A. Kitt, C. W. Magnuson, Y. F. Hao, S. Ahmed, J. H. An, A. K. Swan, B. B. Goldberg, and R. S. Ruoff, *ACS Nano* **5**, 6916 (2011).
- ³²C. R. Dean, A. F. Young, I. Meric, C. Lee, L. Wang, S. Sorgenfrei, K. Watanabe, T. Taniguchi, P. Kim, K. L. Shepard, and J. Hone, *Nat. Nanotechnol.* **5**, 722 (2010).
- ³³R. A. Potyrailo and V. M. Mirsky, *Chem. Rev.* **108**, 770 (2008).
- ³⁴B. Kumar, K. Min, M. Bashirzadeh, A. B. Farimani, M. H. Bae, D. Estrada, Y. D. Kim, P. Yasaei, Y. D. Park, E. Pop, N. R. Aluru, and A. Salehi-Khojin, *Nano Lett.* **13**, 1962 (2013).
- ³⁵A. Hierlemann and R. Gutierrez-Osuna, *Chem. Rev.* **108**, 563 (2008).
- ³⁶F. Rock, N. Barsan, and U. Weimar, *Chem. Rev.* **108**, 705 (2008).
- ³⁷K. Persaud and G. Dodd, *Nature* **299**, 352 (1982).
- ³⁸S. Romyantsev, G. X. Liu, M. S. Shur, R. A. Potyrailo, and A. A. Balandin, *Nano Lett.* **12**, 2294 (2012).
- ³⁹J. Goschnick, *Microelectron. Eng.* **57–58**, 693 (2001).
- ⁴⁰V. V. Sysoev, E. Strelcov, M. Sommer, M. Bruns, I. Kiselev, W. Habicht, S. Kar, L. Gregoratti, M. Kiskinova, and A. Kolmakov, *ACS Nano* **4**, 4487 (2010).
- ⁴¹A. Lipatov, A. Varezchnikov, P. Wilson, V. Sysoev, A. Kolmakov, and A. Sinitskii, *Nanoscale* **5**, 5426 (2013).
- ⁴²V. V. Sysoev, T. Schneider, J. Goschnick, I. Kiselev, W. Habicht, H. Hahn, E. Strelcov, and A. Kolmakov, *Sens. Actuators, B* **139**, 699 (2009).
- ⁴³S. Romyantsev, L. Guanxiong, R. A. Potyrailo, A. A. Balandin, and M. S. Shur, *IEEE Sens. J.* **13**, 2818 (2013).
- ⁴⁴P. C. Jurs, G. A. Bakken, and H. E. McClelland, *Chem. Rev.* **100**, 2649 (2000).
- ⁴⁵D. B. Farmer, R. Golizadeh-Mojarad, V. Perebeinos, Y. M. Lin, G. S. Tulevski, J. C. Tsang, and P. Avouris, *Nano Lett.* **9**, 388 (2009).
- ⁴⁶A. Sinitskii, A. Dimiev, D. A. Corley, A. A. Fursina, D. V. Kosynkin, and J. M. Tour, *ACS Nano* **4**, 1949 (2010).